

# Electrochemical Performance of Synthesized ZnS Microspheres for Super capacitor Applications

Sunil Kumar<sup>a</sup>, Vinay Kumar<sup>a\*</sup>, Sarita Sindhu<sup>a</sup>, Mamta Bulla<sup>a</sup>, Raman Devi<sup>b</sup> & Lalit Kumar<sup>c</sup>

<sup>a</sup>Department of Physics, CCS Haryana Agricultural University, Hisar, Haryana 125 004, India

<sup>b</sup>Institute Instrumentation Centre, Indian Institute of Technology, Roorkee, Uttarakhand 247 667, India

<sup>c</sup>Department of Physics, Meerut College Meerut, Uttar Pradesh 125 004, India

*Received 3 October 2024; accepted 10 February 2025*

The integrated energy conversion and storage mechanism are highly needed in future to fulfil the demand of energy consumption. The current investigation carried out to explore such a material which have immense potential in this sector. The present study explores the electrochemical charge storage behaviour of Zinc Sulphide (ZnS) as supercapacitor electrode. The synthesis was done via cost-effective, efficient, and straight forward reflexive method. The synthesized ZnS nanoparticle exhibit excellent crystallinity with 17 nm of average crystallite size and having microsphere morphology conveyed an excellent specific capacitance of  $74 \text{ Fg}^{-1}$  at  $1 \text{ Ag}^{-1}$  of current density and  $72 \text{ Fg}^{-1}$  at sweep rate of  $1 \text{ mVs}^{-1}$  along with remarkable rate capability that reflects the genuine potential of synthesized ZnS as an electrode for supercapacitor in energy storage.

**Keywords:** Sulfides; Morphology; Specific capacitance; Energy storage

## 1 Introduction

Our day today consumption of energy increased drastically and put extreme pressure on our conventional power supply chain. The conventional power produced by the use of fossil fuels causes serious damage to our environment. As technology is growing day by day it enhances our energy and power consumption but at the same time, these technological advancements have a responsibility to provide the solution to environmental hazards and fulfil our energy demands as well. So sustainable and innovative methods are required for energy conversion and efficient storage of energy. Researchers in this direction try to develop a modern methodology to convert and store energy as per our consumption. Nowadays, the use of renewable energy resources integrated with electrochemical energy storage has proven efficient and sustainable<sup>1,2</sup>.

Supercapacitors (SCs) with higher power density, excellent durability and cyclability have huge potential to build a promising and efficient energy storage mechanism<sup>3</sup>. It is suitable for use in hybrid electric vehicles, portable electronics and renewable energy systems<sup>4,5</sup>. There are two types of SCs that is categorized as electric double layer capacitor

(EDLCs) which store charge electrostatically and pseudocapacitors (PCs), which store and release charges through rapid redox reactions.

The problem with supercapacitors is their lack of energy density<sup>6</sup>, which can be addressed by utilizing pseudocapacitive material with higher specific capacitance and energy density due to faradaic redox reactions than that of EDLCs<sup>7</sup>. Researchers are particularly concerned with different electrode materials as they are deciding element in PCs performance. In comparison to metal oxides, transition metal sulphides (TMS) exhibit exceptional electrochemical performance as they are rich in oxidation states and have higher conductivity, as they are forming with less electronegative element as compared to their oxide counterpart resulting in them being electrochemically useful substances<sup>8</sup>.

Besides all other TMS, ZnS is one of the most important wide band gap semiconductor material. Because of its stability and tunable band gap and morphological features, it has been employed in a number of applications, including sensors, photodetectors, and optoelectronic devices<sup>9</sup>. In general depending on their size, shape, and crystallographic orientations, it comes to light that zinc sulphide exists in two polymorph phases that is wurtzite hexagonal and another one is cubical zinc-

\*Corresponding author: (E-mail: vinay23@hau.ac.in)

blende. Because of its lower energy, the stability of the zinc-blende crystal structure is higher at ambient temperature, while the structure of wurtzite is more persistent above 1000 °C<sup>10</sup>.

ZnS has limited research in the field of electrochemical energy storage sector, despite its exceptional features. ZnS has been extensively studied in opto-electronic devices, such as solar cells, and it can be used to form an integrated system that can function as both energy conversion and storage. Therefore, it would be preferable to synthesize ZnS electrodes with better performance. In this work, ZnS nanoparticles (NP's) with a non-uniform dispersive microspheres shape were effectively produced and used as supercapacitor electrode material. The ZnS electrode has an exceptional rate capability and excellent specific capacitance.

## 2 Materials and Methods

### 2.1 Synthesis of ZnS nanoparticles

The synthesis method for ZnSNP's is displayed in Fig. 1. In a typical procedure, Zinc nitrate hexahydrate (ZNH) is used as a source of zinc ions while thioacetamide (TAA) act as sulphur source. Both the chemicals were dissolved in 30 mL deionized water (DI) separately by rigorously stirring for 10 min, after complete dissolution, the TAA solution was added drop wise using 50 ml burette to the ZNH solution and stirred for another 20 min. that form a transparent solution. This mixture was refluxed at 100 °C for 6h. The obtained yellowish white precipitate of ZnS NP's was centrifuged several times at 6000 rpm using DI water and finally dried at 70 °C for 12 h.

### 2.2 Characterization Techniques

XRD has been used to record the crystal structure and phase determination of ZnS NP's. The functional groups incorporated for the synthesized material were examined using Fourier Transform Infra-Red Spectroscopy (FTIR) and Field Emission Scanning Electron Microscope (FESEM) was employed for assessing the morphology. The Auto lab PG Stat (Metrohm-MAC 204M) with NOVA 2.1.5 software was used for electrochemical analysis. For electrochemical study, a three-electrode setup was employed i.e. ZnS as the working electrode, Ag/AgCl as a reference and platinum wire as the counter electrode.

### 2.3 Electrode fabrication

The working electrode was formed by mixing 32 mg of ZnSNP's with 4 mg of graphite powder and 4 mg of polyvinylidene fluoride (PVDF) in order to analyze the electrochemical performance of the prepared ZnS NP's. Using a magnetic stirrer, this mixture was dissolved in the organic solvent "N-Methyl-2-pyrrolidone" (NMP) and stirred for 6 h to form a consistent slurry. This slurry was cast onto a 1 cm<sup>2</sup> graphite sheet, which served as the current collector (CC) and was then vacuum-dried at 60 °C for a whole night. The CC was loaded with a quantity of 1.21 mg of active material. Using a three-electrode setup the electrochemistry of ZnS nanoparticles was investigated using KOH (6 M) as the electrolyte, Ag/AgCl was used as reference and platinum wire was utilized as a counter electrode.

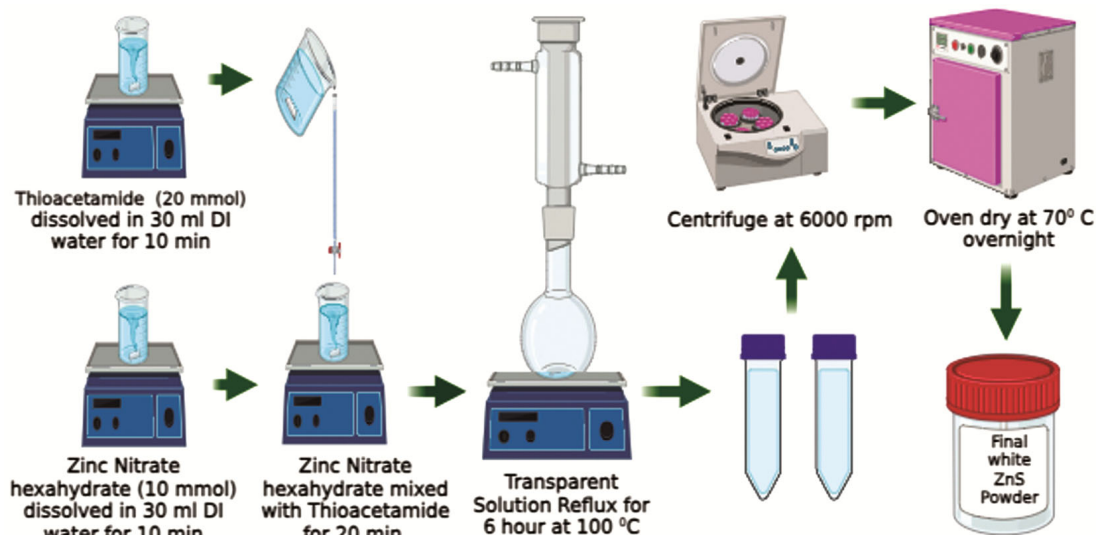


Fig. 1 — Synthesis process of ZnS microspheres

### 3 Results and Discussion

To determine the phase identity and crystallinity of ZnS NP's, the XRD analysis of ZnS powder sample was performed. Fig. 2(a) displays the XRD spectra of synthesized material and the obtained pattern implies that zinc blende cubic phase in ZnS was formed<sup>11</sup>. The XRD spectra shows distinguish peaks at different Bragg's angle. The intense diffracted peaks at  $2\theta$  of  $28.6^\circ$ ,  $33.2^\circ$ ,  $47.6^\circ$ ,  $56.5^\circ$ ,  $69.5^\circ$  and  $76.8^\circ$  were assigned to the (111), (200), (220) (311), (400) and (331) planes respectively that was according to JCPDS card number 36-1450<sup>12</sup> which confirms synthesis of desired NP's with high purity. The crystallite size (D) of the ZnS NP's was obtained by employing the Scherer formula using Eq. (1). The average D value of ZnS NP's was 17 nm obtained using three most intense peak.

$$D = \frac{k\lambda}{\beta \cos\theta} \quad \dots(1)$$

where  $\lambda$  is the wavelength of Cu-K $\alpha$  radiation, k (0.9) is the structure factor,  $\beta$  is the FWHM (Full width at half maxima), and  $\theta$  is the angle of diffraction.

The FTIR spectra of ZnSNP's prepared with the reflux method is depicted in Fig. 2(b). The broad peak around  $3431 \text{ cm}^{-1}$  corresponds to (-OH) stretching while the peak at  $1627 \text{ cm}^{-1}$  corresponds to bending of (H-O-H) group<sup>11</sup>. The S-O bonds formation reflected by peak at  $1112 \text{ cm}^{-1}$  while the peak at  $476 \text{ cm}^{-1}$  confirms the presence of Zn-S bond<sup>13,14</sup>. The absence of peaks in the region of  $400$  to  $460 \text{ cm}^{-1}$  implies that there was no oxidation of zinc ion take place during synthesis process, that gives impurity free ZnSNP's without Zinc oxide<sup>15</sup>.

The surface morphology was examined using FESEM analysis and observation revealed the non-

uniformly distributed sizes of particles as depicted in Figs. 3(a) and (b). It was observed that as prepared ZnSNP's aggregated together and possessed microsphere like morphology as shown in Fig. 3(c). These microspheres consisted of a very fine layer structure (Fig. 3(d)) that plays a crucial role in electrochemical charge storage capability of the prepared material. Due to differences in surface tension and interactive forces during synthesis process, these layers come together and agglomerated microspheres were observed<sup>16</sup>. Fig. 3(e) shows the size distribution of microspheres. Using Image J software, the average size of aggregated NP's was calculated and plotted in a histogram shown in Fig. 3(f) and the average diameter of 381 nm of microspheres was obtained.

#### 3.1 Electrochemical study

Figure 4(a) shows cyclic voltammetry (CV) graphs of ZnS NP's at various sweep rates from 1 to  $50 \text{ mVs}^{-1}$  between -1.0 and 0 V potential window. The excellent pseudocapacitive character of the produced material was indicated by the robust current response and distinct redox peaks displayed by the ZnS electrode. Peak currents increased with the scan rate because of the fast redox reaction brought on by ion diffusion and transfer of charge at the surface of the electrode<sup>17</sup>. The specific capacitance ( $C_s$ ) of prepared electrode examined using Eq. (2).

$$C_s = \frac{\int I dV}{m \times v \times (V_2 - V_1)} \quad \dots(2)$$

where  $\int I dV$  is absolute area of CV plot, v is scan rate,  $(V_2 - V_1)$  is potential window and m is the mass loaded on the CC. The ZnS electrode possesses an excellent  $C_s$  value of  $72 \text{ F g}^{-1}$  at  $1 \text{ mV s}^{-1}$ .

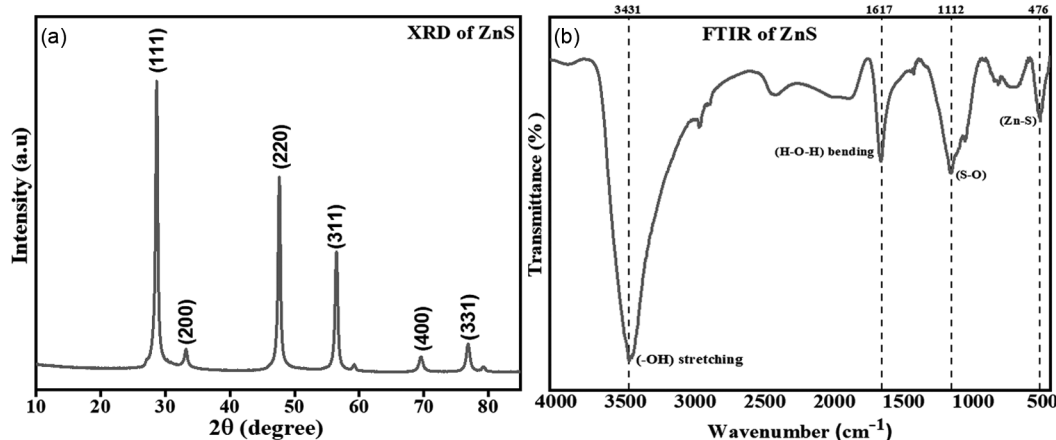


Fig. 2 — (a) XRD pattern of ZnS NP's and (b) FTIR spectra ZnS NP's

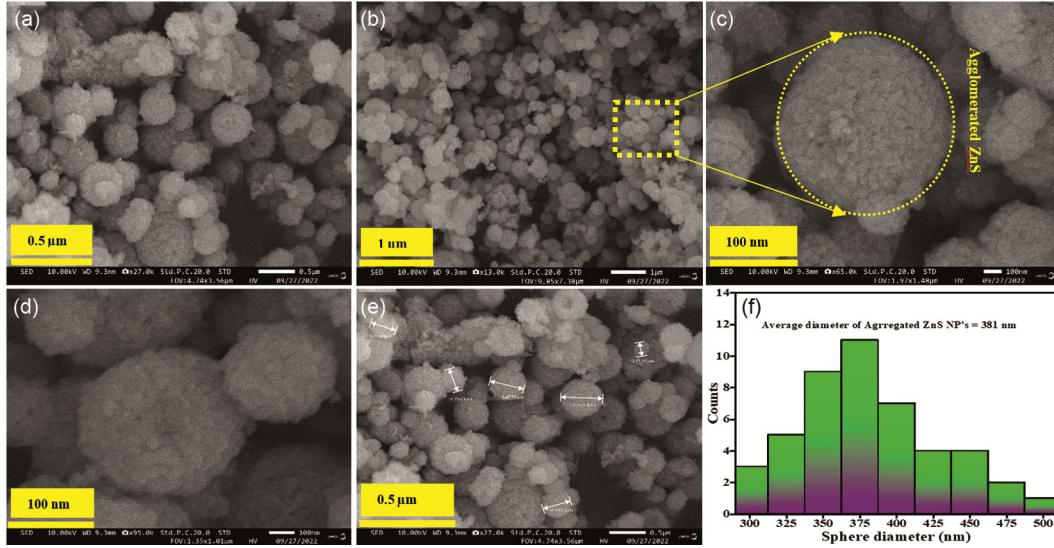


Fig. 3 — (a-e) FESEM micrographs of the ZnS NP's at different magnifications scale and (f) Histogram of size distributions of ZnS NP's

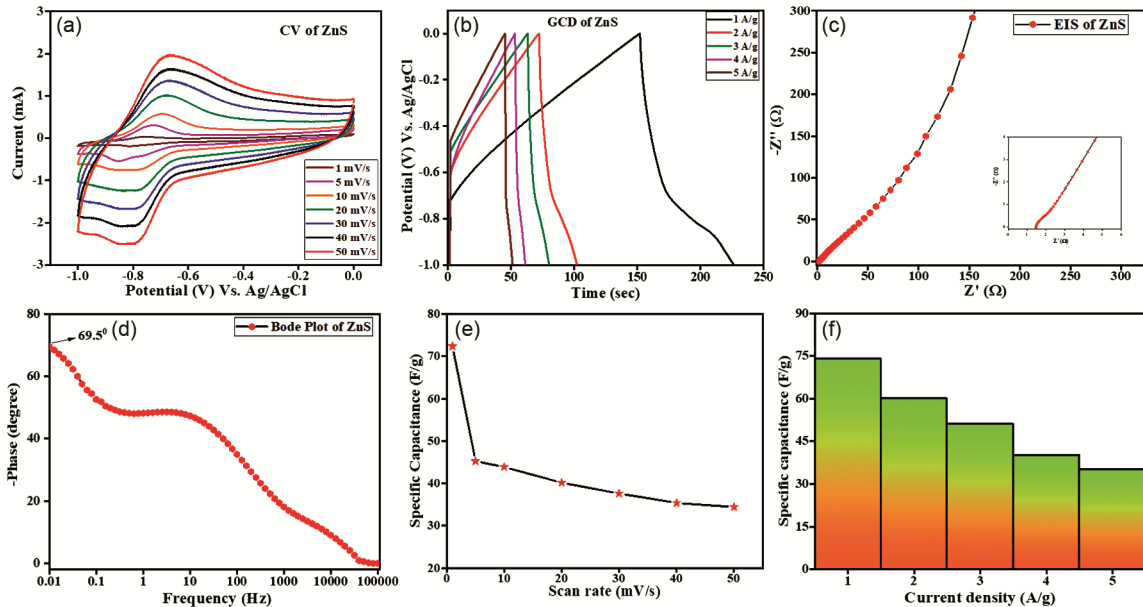


Fig. 4 — (a) CV plot of ZnS (b) GCD profile of ZnS (c) Nyquist plot of ZnS (d) Bode plot of ZnS (e) Specific capacitance v/s scan rate (f) Variation in sp. capacitance v/s current density

The capacitive behaviour was tested by Galvanostatic charge discharge (GCD) that is congruent to the results obtained by CV. Fig. 4(b) displays GCD curves of ZnSNP's at different current densities. The  $C_s$  value of the prepared material was evaluated from GCD by the use of Eq. (3) and it shows remarkable capacitance of  $74 \text{ Fg}^{-1}$  at of  $1 \text{ Ag}^{-1}$ .

$$C_s = \frac{I \times \Delta t}{m \times (V_2 - V_1)} \quad \dots(3)$$

In the above equation,  $I$ ,  $\Delta t$ ,  $m$ , and  $(V_2 - V_1)$  represents current, discharging time, mass deposited on the CC and potential window respectively.

Electrochemical impedance spectroscopy (EIS) was performed for better understanding of the internal dynamics of the electrode and the transmission process of electrolyte ions into the electrode, in the frequency range of 0.01 Hz to 100 kHz. EIS delivers important insights into the kinetics of ion transport, the internal resistances of electrode and the capacitive behavior of electrode material<sup>18</sup>. The Nyquist plot in Fig. 4(c) for ZnS NP's shows a small semi-circular arc (inset of Fig. 4(c)) in the region of high-frequency. The solution resistance ( $R_s$ ) calculated from the curve intersection on real axis ( $Z'$ -axis) and the radius of the

Table 1 — Specific capacitance obtained by CV and GCD

Scan rate (mV s <sup>-1</sup> )	CV		GCD	
	C <sub>s</sub> (F g <sup>-1</sup> )	Current density (A g <sup>-1</sup> )	C <sub>s</sub> (F g <sup>-1</sup> )	Current density (A g <sup>-1</sup> )
1	72	1	74	
5	45	2	60	
10	43	3	51	
20	40	4	40	
30	37	5	35	
40	35			
50	34			

semicircle gives resistance of charge transfers ( $R_{ct}$ ) of the material<sup>19</sup>. The ZnS electrode showed a low  $R_s$  and  $R_{ct}$  value of 1.4  $\Omega$  and 2.3  $\Omega$  respectively that shows the excellent conductivity of electrode and good compatibility of electrode material with KOH electrolyte. In the lower-frequency region, a vertically aligned line with a steep slope indicates remarkable capacitive nature of synthesized material.

The excellent electrochemical capacitive nature of ZnSNP's also reflected with high phase difference of 69.5° (Fig. 4(d)) as shown in bode plot. As seen in Fig. 4(e), the exceptional capacitive performance, even at higher scan rate is a reflection of high rate capability of the electrode material. There is decrease in specific capacitance as we increase the current density as shown in Fig. 4(f) and this happens as ions don't have enough time to explore all active sites of the electrode material and limiting itself only to the outer surface area<sup>12</sup>. The Table 1 shows the capacitance obtained at various scan rate and current densities by CV and GCD techniques.

#### 4 Conclusion

To sum up, ZnS NP's were produced that provides excellent electrochemical performance for supercapacitor. The ZnS NP's electrode exhibits a synergistic effect due to its non-uniform microsphere morphology, with an average microsphere diameter of 381 nm besides its excellent crystallinity with average crystallite size of 17 nm. Additionally, the electrode has an specific capacitance of 74 Fg<sup>-1</sup> at 1 Ag<sup>-1</sup> of current density and 72 Fg<sup>-1</sup> at scan rate of 1 mVs<sup>-1</sup>, with a high rate capability. The current study used a

simple, inexpensive, and energy-efficient chemical method to synthesis ZnS NP's, which provides a viable means of creating innovative and effective integrated energy conversion and storage mechanisms. The potential use of as synthesized ZnS NPs as a leading contender for high-performance energy storage supercapacitor is confirmed by this work.

#### References

- 1 Aricò A S, Bruce P, Scrosati B, Tarascon J M & Van Schalkwijk W, *Nat Mater*, 4 (2005) 366.
- 2 Liu C, Ren Q Q, Zhang S W, Yin B S, Yin L F, Que, Zhao L, Sui F D, Yu X Li, Gu D M & Wang Z B, *Chem Eng J*, 370 (2019) 1485.
- 3 Simon P & Gogotsi Y, *Nat Mater*, 7 (2008) 845.
- 4 Boukhalfa S, Evanoff K & Yushin G, *Energy Environ Sci*, 5 (2012) 6872.
- 5 Gu Y, Fan L Q, Huang J L, Geng C L, Lin J M, Huang M L, Huang Y F & Wu J H, *J Power Sources*, 425 (2019) 60.
- 6 Kumar S, Kumar V, Devi R, Sisodia A K, Jatrana A, Singh R B & Mishra A K, *Adv Mater Sci Eng*, (2022) 1.
- 7 Arul N S, Cavalcante L S & Han J I, *J Solid State Electrochem*, 22 (2018) 303.
- 8 Javed M S, Chen J, Chen L, Xi Y, Zhang C, Wan B & Hu C, *J Mater Chem A*, 4 (2016) 667.
- 9 Hou X, Peng T, Cheng J, Yu Q, Luo R, Lu Y, Liu X, Kim J K, He J & Luo Y, *Nano Res*, 10 (2017) 2570.
- 10 Xiong D, Li X, Bai Z, Li J, Han Y & Li D, *Chem–A Eur J*, 24 (2018) 2339.
- 11 Suganthi G, Arockiadoss T & Uma T S, *Наносистемы: физика, химия, математика*, 7 (2016) 637.
- 12 Hussain I, Mohapatra D, Dhakal G, Lamiel C, Sayed M S, Sahoo S, Mohamed S G, Kim J S, Lee Y R & Shim J J, *J Energy Storage*, 36 (2021) 102408.
- 13 Chlique C, Merdrignac-Conanec O, Hakmeh N, Zhang X & Adam J L, *J Am Ceram Soc*, 96 (2013) 3070.
- 14 Eyasu A, Yadav O P & Bachheti R K, *Int J Chem Tech Res*, 5 (2013) 1452.
- 15 She Y Y, Juan Y A N G & Qiu K Q, *Trans Nonferrous Metal Soc China*, 20 (2010) s211.
- 16 Sihag S, Bulla M, Dahiya R, Bhardwaj N & Kumar V, *Indian J Pure Appl Phys*, 61 (2023) 754.
- 17 Yi T F, Li Y, Li Y M, Luo S & Liu Y G, *Solid State Ionics*, 343 (2019) 115074.
- 18 Yuan Y, Lv H, Xu Q, Liu H & Wang Y, *Nanoscale*, 11 (2019) 4318.
- 19 Devi R, Kumar V, Kumar S, Bulla M & Mishra A K, *J Energy Storage*, 79 (2024) 110167.